

Reentrant Supersolid in the second layer of Helium 4 adsorbed on graphite and Para-Hydrogen adsorbed on Krypton-prelated graphite

Jinwu Ye

Department of Physics, The Pennsylvania State University, University Park, PA, 16802

(January 26, 2020)

We apply the extended boson Hubbard model approach to study (1) hydrogen adsorbed on Krypton-prelated graphite ($H_2/\text{Kr}/\text{graphite}$) near half filling which was investigated in a recent experiment. (2) the reentrant "superfluid" in a narrow region of coverages in the second layer of ^4He adsorbed on graphite detected by a previous torsional oscillator experiment. The transition at zero temperature *driven by the coverage* should be a Commensurate-Charge Density Wave(CDW) at half filling to a narrow window of supersolid, then to an Incommensurate-CDW transition. In the Ising limit, the supersolid is an Ising supersolid (I-SS). While in the easy-plane limit, it is a valence bond supersolid (V-SS). There should be a Kosterlitz-Thouless finite temperature phase transition above which the supersolid becomes a coexistence of CDW and normal fluids of interstitials. We also suggest possible favorable adsorption systems to observe H_2 supersolid.

A superfluid is a fluid that flows through the tiniest channels or cracks without viscosity. So far, the phenomenon of superfluidity has been firmly observed in only two kinds of systems. The first system is in the two isotopes of Helium: ^4He and ^3He which become superfluids below the transition temperatures $T_c = 2.18\text{K}$ and $T_c = 2.4\text{mK}$ respectively [1,2]. Torsional oscillator method was used to study ^4He films adsorbed on graphite [5,6]. Although the ^4He atoms form a triangular lattice at the completion of the first layer, a large Non-Classical Rotational Inertial (NCRI) was detected in a narrow window of coverages in the second layer [5], this important phenomenon was interpreted as reentrant "superfluid" in this narrow window [6,7]. The NCRI is a low temperature reduction in the rotational moment of inertia due to the superfluid component of the state [10]. Recently, also by using the torsional oscillator measurement, a PSU group lead by Chan observed a marked 1 ~ 2% NCRI even in bulk solid ^4He at $\sim 0.2\text{K}$ [8]. This was interpreted as a new state of matter called supersolid which has both superfluid order and crystalline order [8,9]. However, so far, no NCRI in bulk solid H_2 was discovered [11]. The second system is realized in Bose-Einstein condensation in ultra-cold alkali atomic gases (for a review, see [3]). Superfluid to Mott insulator transition was also observed in optical lattices of ultra-cold alkali atoms [12]. There are great interests in finding superfluidity in other light quantum gases such as the isotopes of molecular hydrogen (H_2 , HD and D_2), because of its abundance in nature. Hydrogen molecules are relatively light, quantum fluctuations are large at very low temperature, so they could become superfluids at low enough temperature as ^4He does. Unfortunately, unlike ^4He , due to deeper attractive potentials, bulk H_2 solidifies at $T < T_c \sim 14\text{K}$, this preempts the possible observation of the speculated superfluidity. An important direction is how to create a favorable environment to observe the H_2 superfluid. Obviously, there is no chance to see the bulk H_2 superfluid by tuning temperature or

pressure. One may try to tune other parameters to coax H_2 into a regime which favors superfluid over solid. One potential avenue to prevent $p - H_2$ from being solidified to low enough temperature such that the superfluid behavior can be observed is by the reduction of dimensionality which *decreases* the average number of neighbors of a H_2 . Therefore, extensive theoretical and experimental work has been devoted to study H_2 and D_2 adsorptions in a variety of substrates [13]. In a recent experiment, neutron scattering measurements were used to characterize all the possible phases of D_2 coadsorbed on graphite prelated by a monolayer of Kr called $D_2/\text{Kr}/\text{graphite}$ structure [4]. In the coverage c versus the temperature T phase diagram, an unusual feature is that in a small coverage range ($1.20 < c < 1.25$) at the commensurate-incommensurate (C-IC) transition, a reentrant "fluid" phase squeezes in between the C and IC phases down to $T = 1.5\text{K}$ which is the lowest temperature a liquid-like phase of D_2 has ever been found [4]. The reason that D_2 instead of $p - H_2$ (which has larger de Boer quantum number than D_2) was used in the experiment is that D_2 has a much larger *coherent* neutron-scattering cross-section than that of H_2 . The preferred adsorption sites of a bare graphite substrate form a triangular lattice. Due to the strong corrugate potential of the substrate, at a suitable filling factor which was defined $c = 1$ [4], the H_2 molecules adsorbed on the graphite basal plane may take one of the three sublattices of the triangular lattice to form a $\sqrt{3} \times \sqrt{3}R30^\circ$ structure with the lattice constant $a \sim 4.26\text{\AA}$. In the experiment [4], the precoated Kr atoms will form a triangular lattice which is *incommensurate* with the underlying graphite substrate and sits at the height $z \sim 3.5\text{\AA}$ above the graphite substrate. Then the H_2 deposited on top of the Kr monolayer will sit on the preferred adsorption sites of the triangular lattice of the Kr monolayer which form a honeycomb lattice which sits at the height $z \sim 7\text{\AA}$ above the graphite substrate (Fig.1). Namely, the *Kr* spacer changes the symmetry of the array of adsorption sites from a triangular lattice on

bare graphite to a honeycomb lattice. The coordination number of the honeycomb lattice is $Z = 3$ which is the smallest coordination number one can achieve in a two-dimensional lattice, so it has the best chance to observe the possible superfluid state of H_2 . The filling factor f is related to the coverage c of H_2 with $c = 1.2$ corresponding to $f = 1/2$ where one H_2 molecule occupies every two lattice sites of the honeycomb lattice with $d_{AA} \sim 3.87\text{\AA}$ and $d_{AB} \sim 2.24\text{\AA}$.

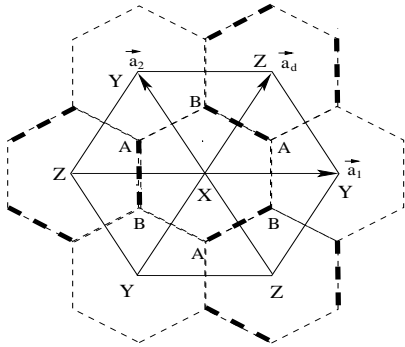


Fig 1: Kr atoms preplated on graphite form a triangular lattice (solid line) which is *incommensurate* with the underlying graphite substrate (not shown in the Fig.). It has three sublattices X, Y, Z . H_2 molecules deposited on top of the Kr monolayer sit in its dual lattice which is a honeycomb lattice (dashed line). It has two sublattices A and B . In the easy-plane limit, one of the three VBS states is shown in the figure, the thick dashed bond is twice as strong as that of thin dashed bond. The other two VBS can be obtained by $R_{2\pi/3}^A$ or $R_{2\pi/3}^B$. The lattice structures may also be relevant to the second layer 4He adsorption on graphite.

In this paper, we will use the extended boson-Hubbard model Eqn.1 on honeycomb lattice to study this possible reentrant "fluid" phase and the reentrant "superfluid" in the second layer of the 4He films adsorbed on graphite. We find a reentrant supersolid (SS) state is a generic state sandwiched between the C-IC transition. The "fluid" like state in the first system is a H_2 supersolid at $T = 0$, while the reentrant "superfluid" state is a 4He supersolid.

The Extended Boson Hubbard model with various kinds of interactions, on all kinds of lattices and at different filling factors is described by the following Hamiltonian [14]:

$$\begin{aligned}
 H = & -t \sum_{\langle ij \rangle} (b_i^\dagger b_j + h.c.) - \mu \sum_i n_i + \frac{U}{2} \sum_i n_i(n_i - 1) \\
 & + V_1 \sum_{\langle ij \rangle} n_i n_j + V_2 \sum_{\langle\langle ik \rangle\rangle} n_i n_k + \dots \quad (1)
 \end{aligned}$$

where $n_i = b_i^\dagger b_i$ is the boson density, t is the nearest neighbor hopping amplitude. U, V_1, V_2 are onsite, nearest neighbor (nn) and next nearest neighbor (nnn) interactions respectively, the \dots may include further neighbor interactions and possible ring-exchange interactions.

The Eqn.1 with only the onsite interaction was first studied in Ref. [14]. The effects of long range Coulomb interactions on the transition was studied in [15]. Very recently, the most general cases Eqn.1 in square lattice at generic commensurate filling factors $f = p/q$ (p, q are relative prime numbers) were systematically studied in [16]. After performing the charge-vortex duality transformation, the authors in [16] obtained a dual theory of Eqn.1 in term of the interacting vortices ψ_l hopping on the dual lattice subject to a fluctuating "dual" magnetic field". The average strength of the dual "magnetic field" through a dual plaquette is equal to the boson density $f = p/q$. This is similar to the Hofstadter problem of electrons moving in a crystal lattice in the presence of a magnetic field [18]. The magnetic space group (MSG) in the presence of this dual magnetic field dictates that there are at least q -fold degenerate minima in the mean field energy spectrum. The q minima can be labeled as $\psi_l, l = 0, 1, \dots, q-1$ which forms a q dimensional representation of the MSG. In the continuum limit, the final effective theory describing the superconductor to the insulator transition in terms of these q order parameters should be invariant under this MSG.

The dual approach is a MSG symmetry-based approach which can be used to classify all the possible phases and phase transitions. Unfortunately, like any other group theoretical approach, if a particular phase will appear or not as a ground state can not be addressed in this approach, it depends on the specific values of all the possible parameters in the boson Hubbard model in Eqn.1. There are two ways to remedy this short-coming. (1) we can compare our theoretical classifications with some known phases observed in experiments, then we can be more specific on our predictions on the nature of *unknown* phases and phase transitions. (2) A microscopic approach such as Quantum Monte-Carlo (QMC) [20] may be needed to supplement the dual field theoretical approach. The dual approach can guide the QMC to search for particular phases and phase transitions in a specific model. In the following, we will take the first strategy to study the boson Hubbard model Eqn.1 in honeycomb lattice at $q = 2$ (Fig.1). We will also compare our results with previous QMC results on square lattices.

When applying the Eqn.1 to the $H_2/Kr/graphite$ system in Fig.1, b_i is the hydrogen molecule creation operator. Because of the Kr spacer, the corrugate of the graphite acting on the H_2 at the height $z \sim 7\text{\AA}$ is sufficiently weak and can be ignored, so t is determined by the trapping potential depth of the Kr triangular lattice which should be considerably larger than that on bare graphite. μ is the chemical potential which determines the coverage. We assume the H_2 molecules interact with each other with the Lennard-Jones (LJ) potential with the parameter $\sigma_{H_2} \sim 2.7\text{\AA}$. Note that the LJ potential is quite accurate in describing the long distance attractive part, but very crude in the short distance repulsive part.

The repulsive part in real case is expected to be much softer. The onsite U is very big. Because $d_{AB} < \sigma_{H_2}$, so V_1 could also be big and positive, it can be considerably reduced due to the phenomenon of rumpling where the optimal height of the B sublattice sites z_B is slightly higher than that of A sublattice sites z_A by a few tenth of \tilde{A} [19]. If the rumpling indeed happens, then the honeycomb lattice symmetry is only approximate. Because $d_{AA} > \sigma_{H_2}$, so V_2 and further neighbor interactions are weakly attractive.

The dual lattice of the honeycomb lattice is a triangular lattice. Two basis vectors of a primitive unit cell of the triangular lattice can be chosen as $\vec{a}_1 = \hat{x}, \vec{a}_2 = -\frac{1}{2}\hat{x} + \frac{\sqrt{3}}{2}\hat{y}, \vec{a}_d = \vec{a}_1 + \vec{a}_2$ as shown in Fig.1. The reciprocal lattice of a triangular lattice is also a triangular lattice and spanned by two basis vectors $\vec{k} = k_1\vec{b}_1 + k_2\vec{b}_2$ with $\vec{b}_1 = \hat{x} + \frac{\hat{y}}{\sqrt{3}}, \vec{b}_2 = \frac{2}{\sqrt{3}}\hat{y}$ satisfying $\vec{b}_i \cdot \vec{a}_j = \delta_{ij}$. The point group of a triangular lattice is $C_{6v} \sim D_6$ which contains 12 elements. The two generators can be chosen as $C_6 = R_{\pi/3}, I_1$. The space group also includes the two translation operators along \vec{a}_1 and \vec{a}_2 directions T_1 and T_2 . In order to derive the MSG, it is enough to look at the mean field vortex hopping Hamiltonian, because the AB phase factors only appear in the kinetic term Eqn.2, *any vortex interactions will commute with the generators of the MSG constructed solely from the kinetic term*. In the Landau gauge $\vec{A} = (0, Hx)$, the Hofstadter Hamiltonian for the vortices hopping in a triangular lattice in the presence of f flux quanta per triangle in the tight-binding limit is:

$$\begin{aligned} \mathcal{H}_v = & -t_v \sum_{\vec{x}} [|\vec{x} + \vec{a}_1 \rangle \langle \vec{x}| + h.c. \\ & + |\vec{x} + \vec{a}_2 \rangle \langle \vec{x}| + h.c. \\ & + |\vec{x} + \vec{a}_d \rangle \langle \vec{x}| + h.c.] \end{aligned} \quad (2)$$

where t_v is the vortex hopping amplitude and $\vec{x} = a_1\vec{a}_1 + a_2\vec{a}_2$ denotes lattice points of the triangular lattice.

The 3 translation operators T_1, T_2, T_d , the rotation operator $R_{\pi/3}$, the 3 reflection operators I_1, I_2, I_d , the two rotation operators around the direct lattice points A and B : $R_{2\pi/3}^A, R_{2\pi/3}^B$ of the MSG of Eqn.2 are worked out in [19]. It can be shown that they all commute with \mathcal{H}_v . However, they do not commute with each other, for example, $T_1T_2 = \omega T_d, T_1T_2 = \omega^2 T_2T_1$ where $\omega = e^{i2\pi f}$.

In the following, we focus on $q = 2$ case where there is only *one* band $E(\vec{k}) = -2t(\cos k_1 + \cos k_2 - \cos(k_1 + k_2))$. Obviously, $E(k_1, k_2) = E(-k_1, -k_2) = E(k_2, k_1)$. There are *two* minima at $\vec{k}_{\pm} = \pm(\pi/3, \pi/3)$. Let's label the two eigenmodes at the two minima as $\psi_{a/b}$. We find the two fields transform under the MSG as [19]:

$$\begin{aligned} T_1, T_2 : \psi_{a/b} & \rightarrow e^{\mp i\pi/3} \psi_{a/b}; & T_d : \psi_{a/b} & \rightarrow -e^{\mp i2\pi/3} \psi_{a/b} \\ R_{\pi/3} : \psi_{a/b} & \rightarrow \psi_{b/a}; & I_{\alpha} \psi_{a/b} & \rightarrow \psi_{b/a}^*, \quad \alpha = 1, 2, d \\ R_{2\pi/3}^A : \psi_{a/b} & \rightarrow e^{\mp i\pi/3} \psi_{a/b}; & R_{2\pi/3}^B : \psi_{a/b} & \rightarrow e^{\pm i\pi/3} \psi_{a/b} \end{aligned} \quad (3)$$

where the transformations under $T_{\alpha}, R_{\pi/3}$ were already derived in [16].

Moving *slightly* away from half filling $f = 1/2$ corresponds to adding a small *mean* dual magnetic field $H \sim \delta f = f - 1/2$ in the action. It can be shown that the most general action invariant under all the transformations in Eqn.3 upto quartic terms is [19]:

$$\begin{aligned} \mathcal{L} = & \sum_{\alpha=a/b} |(\partial_{\mu} - iA_{\mu})\psi_{\alpha}|^2 + r|\psi_{\alpha}|^2 + \frac{1}{4}(\epsilon_{\mu\nu\lambda}\partial_{\nu}A_{\lambda} - 2\pi\delta f\delta_{\mu\tau})^2 \\ & + \gamma_0(|\psi_a|^2 + |\psi_b|^2)^2 - \gamma_1(|\psi_a|^2 - |\psi_b|^2)^2 + \dots \end{aligned} \quad (4)$$

where A_{μ} is a non-compact $U(1)$ gauge field. Upto the quartic level, Eqn.4 is the same as that in the square lattice derived in [16].

Because the duality transformation is a non-local transformation, the relations between the phenomenological parameters in Eqn.4 and the microscopic parameters in Eqn.1 are highly non-local and not known. In fact, the experimental values of the microscopic parameters themselves are not precisely known anyway in the first place. Fortunately, we are still able to classify all the possible phases and phase transitions from Eqn.4 without knowing these relations. If $r > 0$, the system is in the superfluid state $\langle \psi_l \rangle = 0$ for every $l = a/b$. If $r < 0$, the system is in the insulating state $\langle \psi_l \rangle \neq 0$ for at least one l . In any *supersolid* state, one condenses a vortex-antivortex pair, but still keeps $\langle \psi_l \rangle = 0$ for every l . In the insulating or supersolid states, there must exist some kinds of charge density wave (CDW) or valence bond solid (VBS) states which may be stabilized by longer range interactions or possible ring exchange interactions in Eqn.1. Up to an unknown prefactor [19], we can identify the boson densities on sites A and B and the boson kinetic energy on the link between A and B which are the order parameters for the CDW and VBS respectively as $\rho_A = \psi_a^{\dagger}\psi_a, \rho_B = \psi_b^{\dagger}\psi_b$ and $K_{AB} = e^{i\vec{Q}\cdot\vec{x}}\psi_a^{\dagger}\psi_b + e^{-i\vec{Q}\cdot\vec{x}}\psi_b^{\dagger}\psi_a$ where $\vec{Q} = 2\pi/3(1, 1)$ and \vec{x} stands for dual lattice points *only*.

We assume $r < 0$ in Eqn.4, so the system is in the insulating state. In the following, we discuss the the Ising limit first, then the easy-plane limit. If $\gamma_1 > 0$, the system is in the Ising limit, the mean field solution is $\psi_a = 1, \psi_b = 0$ or vice versa. The system is in the CDW order. Setting $\psi_b = 0$ in Eqn.4 leads to:

$$\begin{aligned} \mathcal{L}_I^a = & |(\partial_{\mu} - iA_{\mu})\psi_a|^2 + r|\psi_a|^2 + u|\psi_a|^4 + \dots \\ & + \frac{1}{4}(\nabla \times \vec{A} - 2\pi\delta f)^2 \end{aligned} \quad (5)$$

where $\rho_A = \psi_a^{\dagger}\psi_a$ should be interpreted as the vacancy number, while its vortices are interpreted as boson number.

Eqn.5 has the structure identical to the conventional $q = 1$ component Ginzburg-Landau model for a "superconductor" in a "magnetic" field. For type II superconductors, at mean field level, there is a direct 1st

order transition between the Meissner and the vortex-lattice phase. However, as shown in [21], the gauge field fluctuations will render the vortex fluid phase intruding at H_{c1} between the two phases. Namely, the mean field 1st order transition splits into two 2nd order transitions. For parameters appropriate to the cuprate superconductors, this intrusion occurs over too narrow an interval of H to be observed in experiments. In the present boson problem with the nearest neighbor interaction $V_1 > 0$ in Eqn.1 which stabilizes the CDW state at $f = 1/2$, this corresponds to a Ising supersolid (I-SS) state intruding between the commensurate CDW state at $f = 1/2$ and the in-commensurate CDW state at $1/2 + \delta f$ as shown in Fig.2a. We expect the intruding window at our $q = 2$ system is much wider than that of the $q = 1$ system. In the I-SS state, $\langle \psi_a \rangle = \langle \psi_b \rangle = 0$, but $\langle \psi_a^\dagger \psi_a \rangle \neq 0$, $\langle \psi_b^\dagger \psi_b \rangle = 0$, so there is a (π, π) diagonal order and superfluid density $\rho_s \sim \delta f$. There is a 2nd order transition from the I-SS to the superfluid inside the window driven by the quantum fluctuation r in the Fig.2a. All the 2nd order transitions are in the 3D XY universality class.

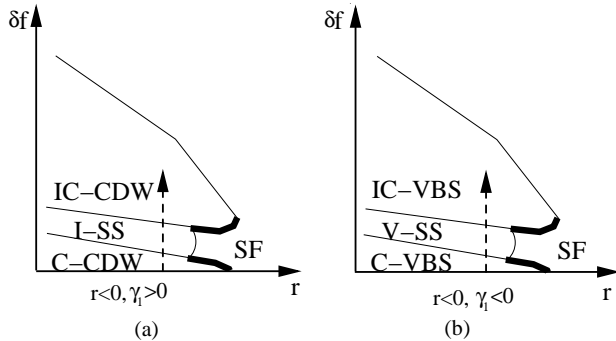


Fig 2: The zero temperature phase diagram of the chemical potential μ versus r in Eqn.4 in (a) The Ising limit $\gamma_1 > 0$ and (b) the Easy-Plane limit $\gamma_1 < 0$. (a) There is a Ising Supersolid (I-SS) state intruding between the commensurate CDW (C-CDW) state at $f = 1/2$ and the in-commensurate CDW (IC-CDW) state at $1/2 + \delta f$. (b) There is a Valence Bond Supersolid (V-SS) state intruding between the commensurate VBS (C-VBS) state at $f = 1/2$ and the in-commensurate VBS (IC-VBS) state at $1/2 + \delta f$. The dashed line is the experimental path in $D_2/Kr/graphite$ or in the second layer of 4He adsorbed on graphite at $T = 0$ [22]. The thin (thick) line is the 1st (2nd) order transition. All the 2nd order transitions are in the 3D XY universality class.

Fig.2a is very similar to the $c \sim f$ versus low T phase diagram in $H_2/Kr/graphite$ structure near $c = 1.20$ (Fig. 6 in [4]). The so called $(1 \times 1)_{\lfloor \frac{1}{2} \rfloor}$ commensurate phase in [4] is the CDW state where the D_2 atoms occupy one of the two sublattices of the underlying honeycomb lattice. There is a finite temperature Ising transition above this phase. The transition at zero temperature is a C-CDW to I-SS to IC-CDW transition described by Eqn.4 in the Ising limit $r < 0, \gamma_1 > 0$. Obviously, it is very difficult

to reach the superfluid by moving along the horizontal r axis, but it is very easy to get to the I-SS state by moving along the vertical coverage axis. If this is indeed the case, this may lead to the first observation of H_2 supersolid. There should be a Kosterlitz-Thouless (KT) finite temperature phase transition above which the I-SS becomes a coexistence of the CDW state and normal fluids of interstitials. Unfortunately, this finite KT transition was not observed in Fig.6 in [4] until to $1.5K$. This is certainly expected, because, due to the tiny fraction of superfluid density of the I-SS, the T_{KT} is very small. So the " fluidlike " state claimed in the experiment in [4] can only the coexistence which may not shown any neutron scattering peaks.

If $\gamma_1 < 0$, the system is in the easy-plane limit. It is unlikely to reach the easy-plane limit in the H_2 system because of the smaller de Boer quantum number. However, it may be possible to reach this limit in the 4He system. At $q = 2$, the mean field solution is $\psi_a = e^{i\theta_a}, \psi_b = e^{i\theta_b}$. $\rho_A = \rho_B = 1$, so the two sublattices remain equivalent. The system has VBS order. The kinetic energy $K_{AB} = \cos(\vec{Q} \cdot \vec{x} + \theta_-)$ where $\theta_- = \theta_a - \theta_b$. Up to the quartic order, the relative phase between ψ_a and ψ_b is undetermined. Higher order terms are needed to determine the relative phase. It is clear to see there are only 3 sixth order invariants: $C_1 = |\psi_a|^6 + |\psi_b|^6, C_2 = (|\psi_a|^2 + |\psi_b|^2)|\psi_a|^2|\psi_b|^2, C_3 = (\psi_a^* \psi_b)^3 + (\psi_b^* \psi_a)^3 = \lambda \cos 3\theta_-$. Obviously, only the last term C_3 can fix the relative phase. It was shown in [19], both signs of λ are *equivalent*, in sharp contrast to the square lattice where the two signs of $C_{sq} = \lambda \cos 4\theta$ lead to either Columnar dimer or plaquette pattern. One VBS with $\lambda > 0, \theta_- = \pi$ was shown in Fig.1. The other two VBS states can be obtained by $R_{2\pi/3}^{A/B}$. In contrast to the square lattice where C_{sq} is irrelevant near the QCP, C_3 may be relevant, so the transition from the SF to the VBS in Fig.2b could be a 1st order transition instead of a 2nd order deconfined QCP in a square lattice.

Slightly away from the half-filling, Eqn.4 becomes:

$$\begin{aligned} \mathcal{L}_{EP} = & \left(\frac{1}{2}\nabla\theta_+ - \vec{A}\right)^2 + \frac{1}{4}(\nabla \times \vec{A} - 2\pi\delta f)^2 + \dots \\ & + \left(\frac{1}{2}\nabla\theta_-\right)^2 + 2\lambda \cos 3\theta_- \end{aligned} \quad (6)$$

where $\theta_{\pm} = \theta_a \pm \theta_b$.

Obviously, the θ_- sector is massive (namely, θ_a and θ_b are locked together) and can be integrated out. Assuming $\lambda > 0$, then $\theta_- = \pi$. Setting $\psi_+ = e^{i\theta_+} \sim \psi_a \sim -\psi_b$ simplifies the above Eqn. to:

$$\begin{aligned} \mathcal{L}_{EP}^+ = & |(\partial_\mu - iA_\mu)\psi_+|^2 + r|\psi_+|^2 + u|\psi_+|^4 + \dots \\ & + \frac{1}{4}(\nabla \times \vec{A} - 2\pi\delta f)^2 \end{aligned} \quad (7)$$

Again, Eqn.7 has the structure identical to the conventional $q = 1$ Ginzburg-Landau model for a " superconductor " in a " magnetic " field. The discussions on Ising

limit case following Eqn.5 also apply. In the present boson problem with the nearest neighbor interaction $V_1 > 0$ in Eqn.1 which stabilizes the VBS state at $f = 1/2$, this corresponds to a VBS supersolid (V-SS) state intruding between the commensurate VBS (C-VBS) state at $f = 1/2$ and the in-commensurate VBS (IC-VBS) state at $1/2 + \delta f$ as shown in Fig.2b. In this IC-VBS state, δf valence bonds shown in Fig.1 is slightly stronger than the others. In the V-SS state, $\langle \psi_a \rangle = \langle \psi_b \rangle = 0$, but $\langle \psi_a^\dagger \psi_a \rangle = \langle \psi_b^\dagger \psi_b \rangle = -\langle \psi_a^\dagger \psi_b \rangle \neq 0$, so there is a VBS order $K_{AB} = \cos(\vec{Q} \cdot \vec{x} + \theta_-)$, the superfluid density $\rho_s \sim \delta f$. There is a 2nd order transition from the V-SS to the superfluid where $\langle \psi_a \rangle = \langle \psi_b \rangle = 0$ and $\langle \psi_a^\dagger \psi_b \rangle = 0$ inside the window driven by the quantum fluctuation r in the Fig.2. Again, all the 2nd order transitions are in the 3D XY universality class.

A recent Path Integral Monte Carlo (PIMC) simulation [23] on a simplified model of p-H₂/Kr/graphite system found only two stable phases the C-CDW and the IC-CDW, there is a direct first order transition between the two stable phases. In fact, this result is consistent with the mean field result of Eqn.4. However, the gauge field fluctuations ensure that a supersolid phase must intrude between the two phases. Our results are consistent with the QMC simulations in [20] which also reported I-SS on square lattice slightly away from half filling. It is important to perform QMC simulations on honeycomb lattice to confirm the phase diagram Fig.2 in both Ising and easy-plane limit.

In fact, Kr may not be the best spacer to observe this supersolid state. The ideal situation is to make d_{AB} is just smaller than σ_{H_2} . Larger atoms like Xe, CF_4, SF_6 may be more suitable spacers, because they may increase the distance d_{AB} in the Fig.1 very close to σ_{H_2} .

In the experiment of the ⁴He films adsorbed on graphite, the ⁴He atoms form a triangular lattice at the completion of the first layer which is also incommensurate with the underlying graphite. Because the first layer acting as a spacer, the corrugate potential of the graphite acting on the ⁴He in the second layer is sufficiently weak and can be ignored, so the t in Eqn.1 in the second layer should be considerably larger than that in the first layer. Due to the interference between the first and second layer, how the second layer ⁴He register with the first layer is not known. It is reasonable to assume the lattice structure of the preferred adsorption sites on the second layer also form a honeycomb lattice. Then the two systems have the same symmetry and belong to the same universality class, so the above discussions on D₂/Kr/graphite can also be applied. Fig.2a shows that the reentrant "superfluid" detected around $T = 20mK$ in a narrow window of coverages in the second layer of ⁴He films adsorbed on graphite must be the supersolid state. The state after the appearance of the "superfluid" was clearly identified as IC-CDW, but the nature of the

state before the appearance of the "superfluid" can not be clearly identified in the experiment [5], it is reasonable to assume it is a triangular lattice formed by the A sites in Fig.1. Indeed, the data in the torsional oscillator experiment in [5] do not show the characteristic form for a 2d superfluid form, instead it resemble that in [8] characteristic of s supersolid in terms of the gradual onset temperature of the NCRI, the unusual temperature dependence and the independence of the transition temperature T_{SS} on the coverage.

In summary, we applied the dual extended boson Hubbard model approach to investigate all the possible phases in H₂/Kr/graphite near half filling and the reentrant "superfluid" in the second layer of ⁴He adsorbed on graphite. We derive an effective action to describe the quantum phase transition among all the possible phases. We also identified boson density and boson kinetic energy operators to characterize symmetry breaking patterns in the insulating states and supersolid states. We found that the transition at zero temperature *driven by the coverage* must be a C-CDW (or C-VBS) at half filling to a narrow window of supersolid, then to a IC-CDW (IC-VBS) transition in the Ising (easy-plane) limit. In the Ising limit, the supersolid is a Ising supersolid (I-SS). While in the easy-plane limit, it is a valence bond supersolid (V-SS). The Ising limit of the action may describe the coverage versus the low temperature phase diagram near half filling in both systems [4,5]. There should be a KT finite temperature phase transition above which the SS becomes the coexistence of CDW and normal fluids of interstitials. The "fluidlike" state claimed in [4] may be just such a coexistence. H₂/Kr/graphite near half filling is a promising one to search for the first experimental observation of H₂ supersolid at low enough temperature. Torsional oscillator experiment similar to that used in [5] may be used to measure the NCRI of this H₂ supersolid state. Obviously, this experiment can avoid the difficulty of using D₂ which has large coherent neutron scattering cross section, but smaller de Boer quantum number. The reentrant "superfluid" in the 2nd layer detected by the torsional oscillator experiment must be a ⁴He supersolid state. The reentrant lattice SS discussed in this paper is different from the bulk ⁴He SS state discussed in [8,9], although both kinds of supersolids share many interesting common properties. In the former, there is a periodic substrate or spacer potential which breaks translational symmetries at the very beginning. While in the latter, the lattice results from a spontaneous translational symmetry breaking, so the theory developed in this paper on lattices is completely different from the continuum theory developed in [9]. Combined with the results in [8,9,11], we conclude that ⁴He supersolid can exist both in bulk and on substrate, while although H₂ supersolid may not exist in the bulk, but it may exist on substrate.

I am deeply indebted to M. Cole for explaining to me the physics of adatom adsorption on various kinds of sub-

strates. I thank him and Moses Chan for pointing out the experiments in Ref. [4] and Ref. [5] respectively to me. I thank M. Boninsegni, M. Chan, T. Clark, P. A. Crowell, H. Glyde and J. D. Reppy for helpful discussions. This research at KITP was supported in part by the NSF under Grant No. PHY99-07949.

- [1] P. Kapitza, Nature 141, 74 (1938).
- [2] D. D. Osheroff, R. C. Richardson, and D. M. Lee, Phys. Rev. Lett. 28, 885C888 (1972)
- [3] F. Dalfovo, S. Giorgini, L. P. Pitaevskii and S. Stringari, Rev. Mod. Phys. 71, 463C512 (1999).
- [4] H. Wiechert and K. Kortmann, Phys. Rev. B 70, 125410 (2004).
- [5] P. A. Crowell and J. D. Reppy, Phys. Rev. Lett. 70, 3291C3294 (1993)
- [6] P. A. Crowell and J. D. Reppy, Phys. Rev. B 53, 2701C2718 (1996).
- [7] The possibility of supersolid was briefly mentioned in [6]. P. A. Crowell and J. D. Reppy, private communications.
- [8] E. Kim and M. Chan, Nature 427, 225 - 227 (15 Jan 2004); Science 24 September 2004; 305: 1941-1944.
- [9] Jinwu Ye, cond-mat/0604602
- [10] A. J. Leggett, Phys. Rev. Lett. **25**, 1543 (1970).
- [11] M. Chan, private communications.
- [12] M. Greiner, O. Mandel, T. Esslinger, T. W. Hansch, T. Bloch, Nature 415, 39-44 (2002).
- [13] M. C. Gordillo and D. M. Ceperley, Phys. Rev. Lett. 79, 3010 (1997).
- [14] M. P. A. Fisher, P. B. Weichman, G. Grinstein and D. S. Fisher; Phys. Rev. B 40, 546 (1989).
- [15] Jinwu Ye, Phys. Rev. B 58, 9450-9459 (1998).
- [16] L. Balents, L. Bartosch, A. Burkov, S. Sachdev, K. Sengupta, Phy. Rev. B 71, 144508 (2005).
- [17] Longhua Jiang and Jinwu Ye, cond-mat/0601083.
- [18] D. R. Hofstadter, Phys. Rev. B 14, 2239-2249 (1976). J. Zak, Phys. Rev. 134, A1602-A1606 (1964), Phys. Rev. 134, A1607-A1611 (1964).
- [19] Jinwu Ye, unpublished
- [20] G. C. Batroun *et al*, Phys. Rev. Lett. 74, 2527 (1995).
- [21] D. S. Fisher, M. P. A. Fisher and D. A. Huse, Phys. Rev. B 43, 130 (1991).
- [22] When $\delta f = f - 1/2$ is too large, Eqn.4 is not valid anymore. The system may reach C-CDW state at other q .
- [23] J. Turnbull and M. Boninsegni, cond-mat/0503507.